Acta Oceanologica Sinica 2007, Vol. 26, No. 1, p. 55～65
http://www.oceanpress.com.cn
E-mail: hyxbe@263.net

# Measurements of suspended particulate matter with laser in-situ scattering and transmissometry in the Jiaozhou Bay in China

WEI Jianwei[1,2], SHI Xuefa[1,2*], FANG Xisheng[1], ZHANG Weibin[1]

1. First Institute of Oceanography, State Oceanic Administration, Qingdao 266061, China
2. Key Laboratory of Marine Sedimentology and Envriomental Geology of State Oceanic Administration, First Institute of Oceanography, State Oceanic Administration, Qingdao 266061, China

Received 29 January 2006; accepted 10 July 2006

**Abstract**

A laser in-situ scattering and transmissometry probe (LISST-100) was used to estimate the spatial variations of suspended particle (aggregate) distribution, volume concentration and beam attenuation in the Jiaozhou Bay, Qingdao, China on 18 July 2003. One study site was located at the mouth (Sta. J1), with the other being within the inner bay (Sta. J2). Measurements of total suspended matter (TSM) and chlorophyll fluorescence and sampling of bottom sediments were carried out simultaneously. On the basis of the field data, the in-situ particle effective density, settling velocity and flux, and particle projected surface area (PSA) were estimated. The results demonstrate that both profiles have similar particle size distributions from surface to bottom within the water columns. Mean particle diameters for Stas. J1 and J2 are 38～74 and 1～20 μm, respectively, particles within these ranges dominate over the particulate components. Suspended particle volume concentrations increase with water depth, with spikes near the bottom. At Sta. J1, the mean size of bottom sediments and those of suspended particles at 10.8 m below the water surface are almost the same, as well as their size distributions. This observation suggests that a special affinity exists between bottom sediment and suspended particles. In addition, the estimates show that the effective density, settling velocity and flux are higher in the inner bay. Beam attenuation coefficient correlates well with the volume concentration, positively. It is inferred that the optical scattering was mostly caused by 1～250 μm components, among which the particles finer than 20 μm dominate the beam attenuation. The PSA appears a proxy for the leaving reflectance estimation.

**Key words:** suspended particle, size distribution, beam attenuation, LISST-100, Jiaozhou Bay

## 1 Introduction

Knowledge of suspended particle size and distribution is the key elements for better understanding the sediment transport processes (Wang et al., 2004), primary production (Ning et al., 2004), water quality controlling and pollution prediction (Burton et al., 1993; Yang et al., 2004) and even the water color remote sensing (Zhang et al., 2005) in the coastal waters. For many years, the determination of the suspended particle parameters has been a routine of oceanography and environmental evaluation (Sun et al., 2003). However, it cannot be completely ignored that some of the particles exist actually as aggregates (Trent et al., 1978; Bale and Morris, 1986; Eisma et al., 1986), the structures

* Corresponding author, E-mail: xfshi@fio.org.cn

of which are so loose and fragile that they are subject to breakup under ambient stress fields (for example, turbulence). According to Gibbs (1981, 1982) and Gibbs and Konwar (1982, 1983), the traditional methods of water sampling, filtering and even subsequent particle analyzing processes would definitely change the aggregate sizes and modalities. Consequently, measurements with these methods do not describe the in situ particle (aggregate) sizes adequately. This poses some problems for the accurate estimation of grain sizes. To avoid those possible errors, scientists nowadays have been endeavoring to develop and improve the in situ measuring systems for suspended matter sizes, such as video camera system (Sternberg et al., 1999) and laser diffraction technologies (Agrawal and Pottsmith, 1994; Gentien et al., 1995). It should be noted that, Laser In-situ Scattering and Transmissometry (LISST-100) is actually the first multi-parameter underwater particle laser sizer in the world (Agrawal and Pottsmith, 1994), and it can determine the beam attenuation, volume concentration and particle spectrum at the same time. With the state-of-the-art commercial measuring system, it has become possible to measure simultaneously the parameters of particles in an almost non-intrusive manner (Mikkelsen and Pejrup, 2000; Gartner et al., 2001; Mikkelsen, 2002a, 2002b; Voulgaris and Meyers, 2004; Mikkelsen et al., 2005). In past several years, domestic researchers have begun to focus on the application and analysis of in-situ size measurements (Lan et al., 2004; Cheng et al., 2005).

The Jiaozhou bay is a typical tide-controlled and semi-enclosed body of water, lying south of the Shandong Peninsula in China. This area is known as the largest natural harbor, with fast-developing tourism and booming light industries. As ECCB (1993) reported, city garbage and pollutants were discharged into the small bay, as well as modern suspended particles from the seabed and rivers nearby, and also they vary with seasons and localities (Zhang, 2000). As early parts of suspended particle dynamics in coastal waters, a set of LISST-100 system was deployed for evaluation in the Jiaozhou Bay in July 2003. Both in situ suspended particle size data and beam transmission data were obtained for the first time. It is shown how the in situ particle sizes vary with the water depth and how it is possible to estimate the settling velocities and fluxes with the LISST-100 in this study. What is more, the beam attenuation specifically due to particles and their PSA was analyzed. And it indicates the perspectives of LISST-100 in the field of particle dynamics research and optical oceanography study in coastal waters.

## 2 Materials and methods

On 18 July 2003, the underwater in situ particle measurements were carried out at Stas J1 and J2 in the Jiaozhou Bay. Station J1 (36°0.918′N, 120°15.714′E) is located in the outer bay (a new harbor), with a water depth of 13 m and restricted by a narrowing entrance about 3.1 km wide, while Sta. J2 lies at the head of inner bay (36°8.958′N, 120°16.248′E), which is about 6 m deep (Fig. 1). The fieldwork occurred during the high tide period, with force 3 wind.

The LISST-100 used the samll angle forward diffraction principle (Agrawal et al., 1991), to determine the size of suspended particles and the beam attenuaiton. Small-angle scattering, 0.05°～5° in case of LISST-100 type B in this paper, is relatively insensitive to particle composition, and the size distribution meansurements are robust, and do not require particle refractive index. The instrument used in this paper has a 5 cm optical path, and the laser wavelength is 670 nm. A detailed description of the design and operational principles of LISST-100 can be found in Agrawal and Pottsmith (1994), or you may refer to the website of Sequoia Scientific

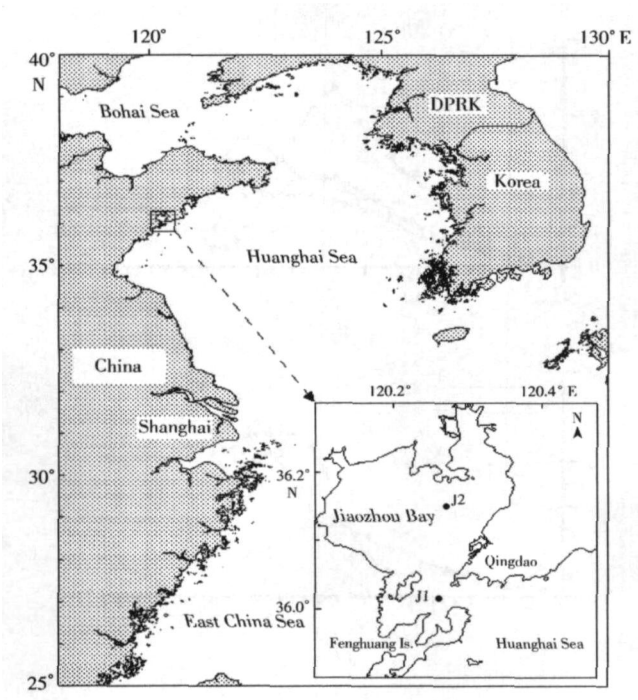


Fig. 1. Locations of the Jiaozhou Bay and the two profiling sites

Inc (http://www.sequoiasci.com). Sampling was carried out with a frequency of 1.1 Hz. The particle size distribution data were stored in 32 logarithmically spaced size classes in the range of 1.25～250 μm. An SBE CT sensor was also interfaced with LISST-100B, from which the water temperature and conductivity could be determined simultaneously.

Before deployment, the background scattering calibration was carried out with distilled water, and compared with the factory background values. If not acceptable, rinse the optial lens very carefully, and another background testing should be repeated until satisfying results come out. Once retrieved, the data were downloaded and then processed into readable ASCII optical scattering and transmission data with LISST software (Agrawal and Pottsmith, 2000). While profiling, water samples were taken with Niskin sampler, and then suction-filtered onto preweighted Whatman GF/F filters, with a nominal retention diameter of 0.7 μm. Upon returning to the onshore laboratory, the filters were oven-dried at 60℃, and weighted with an accuracy of 0.1 mg. The total suspended matter (TSM) could be estimated by subtracting the blanks. Besides, the chlorophyll a fluorescence was profiled with YSI multiparameter sonde by the scientists on board.

## 3 Results

### 3.1 Particle size distributions

Particle size measuring is one of the fundamental functions of LISST-100. Using this system, 32 logrithmatically spaced sizes for Stas. J1 and J2 were obtained in the Jiaozhou Bay. Station J1 has the similar unimodal particle size spectra, with a mode around 32 μm (see Figs. 2a and b). For Sta. J2, the size spectra at 0.25, 1.1 and 2.9 m water deep show an identical trend, with a common fine-grained end and a unimode around 32 μm (see Fig. 2c). And at 4.0 and 4.5 m of the water column at Sta. J2, the size spectra featured a unimode around 80 μm (see Fig. 2d).

### 3.2 Vertical variations in the water column

One to 250 μm suspended particle volume concentration ($c_V$), was obtained by summing all the volume concentrations for 32 size classes divided by the instrument-dependent calibration constant, 4 700 in this case. The particle concentration in the surface waters of Sta. J1 is 17 μL/L, and it sharply increases to 34 μL/L at the bottom. For Sta. J2, the surface volume concentration is about 37 μL/L. And the volume concentration in the waters of 4.5 m is around 70 μL/L, approximately twice that in the surface water. In the deeper waters, the suspended particle concentration is as high as about 150～230 μL/L. It indicates that the J2 profile is much more turbid than J1, especially within the bottom layer. The beam attenuaiton coefficient ($c$) varies

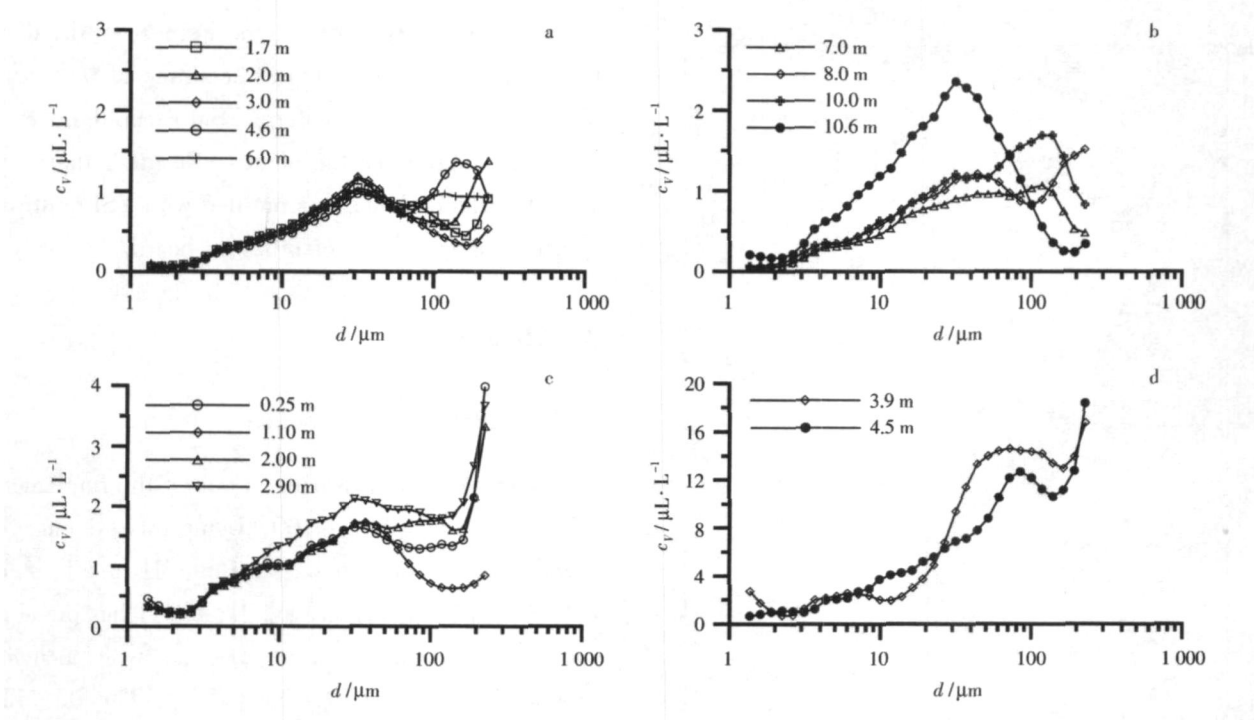


Fig. 2. Variations of suspended particle spectra for the two sites in the Jiaozhou Bay. a and b are the particle size spectra Sta. J1 and c and d show the particle size spectra Sta. J2. $c_V$ is the volume concentration and $d$ is the particle size.

with the particle volume concentrations (Fig. 3). And the strongest attenuation, 25 m$^{-1}$, could be found at the bottom waters.

## 4 Discussion

The system used in this paper is sensitive to the particles within 1～250 μm, and the scattering informaiton can only come out within this range. As for those aggregates or detrital particles larger than 250 μm, their diffraction information would affect the particle distribution, resulting in the "rising tail" at the coarser end of the size spectra. From the foregoing field analysis (Mikkelsen, 2002a; McCandliss et al., 2002; Mikkelsen et al., 2005; Voulgaris and Meyers, 2004), the "rising tail" was a common phenomenon, and would not evidently affact the rigor of the data. In the natural waters, most of the detritus (organic/inorganic) and the phytoplanktons exist in the range of 0.1～250 μm (McCave, 1984). In this sense, the in situ particle scattering informaiton determined by LISST-100B

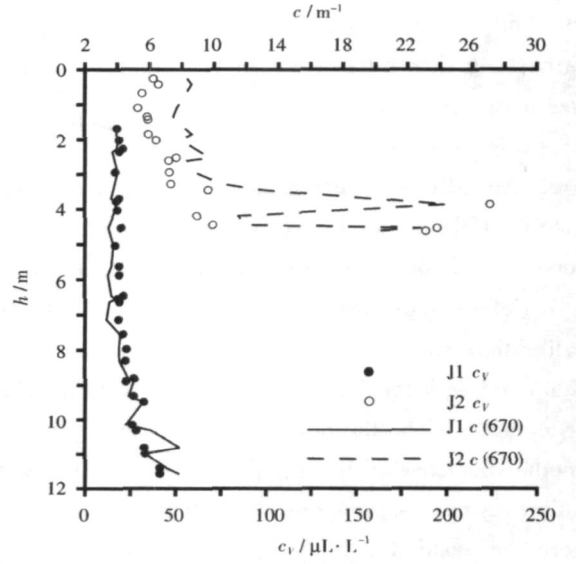


Fig. 3. Variations of suspended particle concentration and beam atteanution coefficient for the two water columns. $h$ is the water depth.

would be reliable to interpret the particle distribution. And it is noted that all the discussions of this paper only referred to the particles within the range of 1～250 μm.

### 4.1 Suspended particle compositions

The suspended particle spectra can be used to trace the particle sources (Kurashige and Fusejima, 1997). Particles with diameters of 1～20 μm dominate the spectra of J1, which account for about 34.2% and 29.5% for the surface (1.7 m) waters and mid-depth (7 m) waters, respectively, and increase to 40.6% at the bottom layer (10.8 m). At Sta. J2, fine particles of 1～20 μm in surface (0.25 m) and bottom (4.4 m) waters account for approximately 34.2% and 29.4%. Very similar size spectra can be found in both profiles, which indicates the possibly same particle sources.

The particle sizes of J1 are coarser than those of J2, and the mean sizes ($d_m$) in the surface waters are much coarser than those in the bottom waters for both profiles (Table 1). Compared with previous reports, it is evident that the in-situ particle size is larger than that from traditional methods. According to the laboratory analysis with Cilas 940L laser particle sizer (Wang et al., 1999), for example, the suspended particle size was found less than 19 μm, the median size was about 1.8 μm and the fine particles of less than 3.6 μm dominate (~65%). Such differences between both kinds of results can be attributed to the mechanical breakage. As a result, the in-situ particle size data actually are covering more realistic environments. In view of biological oceanography, however, living biomass, dead bodies and detritus, and fecal pettlets could contribute to the particle variability. Large particles (aggregates) would come into being in the upper waters which generally have high production.

Table 1. Parameters of the in-situ profiling measurements in the Jiaozhou Bay

| Station | $h$/m | $c_{tsm}$ / mg·dm$^{-3}$ | $c_V$ /μL·L$^{-1}$ 1～250 μm | $c_V$ /μL·L$^{-1}$ 1～20 μm | $d_m$ / μm | $c$/ m$^{-1}$ | $c_p$ / m$^{-1}$ | $A$ / ×10$^{-2}$m$^2$·dm$^{-3}$ | Δρ/ kg·m$^{-3}$ | $w_s$ / mm·s$^{-1}$ | $c_{Chla}$ / mg·m$^{-3}$ |
|---|---|---|---|---|---|---|---|---|---|---|---|
| J1 | 1.7 | 23.5 | 17.95 | 6.13 | 58.1 | 3.92 | 3.542 | 1.709 | 1 309 | 2.400 0 | 2.24 |
| | 7.0 | 34.2 | 18.49 | 5.46 | 62.9 | 6 | 2.946 | 1.479 | 1 850 | 3.977 0 | 1.46 |
| | 10.8 | 40.1 | 32.87 | 13.33 | 38.3 | 3.33 | 7.477 | 3.648 | 1 220 | 0.972 4 | 1.01 |
| J2 | 0.25 | 15.2 | 37.74 | 12.89 | 74.0 | 8.32 | 7.943 | 4.084 | 403 | 1.199 1 | 3.35 |
| | 4.4 | 24.2 | 70.46 | 20.69 | 73.0 | 7 | 11.37 | 6.082 | 343 | - | 2.58 |

Notes: $c_{tsm}$ is total suspended matter, $c_p$ attenuation coefficient resulted from particles, $A$ projected surface area, Δρ effective density, $w_s$ settling volocity, and $c_{Chla}$ chlorophyll a concentration.

One surface sediment sample from Sta. J1 was also analyzed with the Malvern 2000 laser sizer to compare with the suspended particles. One part was dealt with $H_2O_2$ to remove the organic components, while the other was analyzed without any treatment. The results show that the particle diameters for bottom sediments are 0.3～200 μm. And the organic matter is quantitatively negligible (see Fig. 4). The integrated components for 0.3～1.25, 1.25～20 and 100～500 μm size ranges account for 5%, 48% and 6% of bulk sediment samples, respectively. The shape of size spectrum for the bottom sediment is compariative to that of suspended particles. The mean grain size of bottom sediment is 35.86 μm, a little finer than suspended particles (38.3 μm). From the above analysis, an affinity

between suspended matters and bottom sediments could be anticipated.

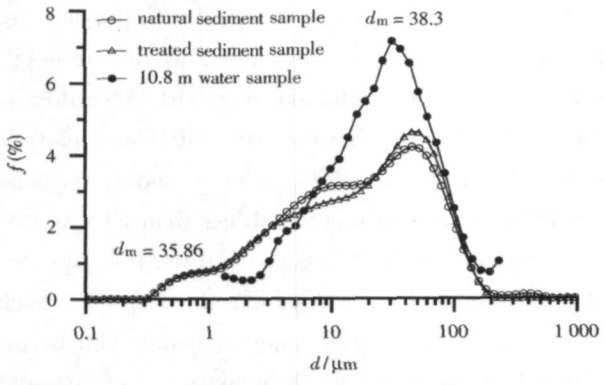


Fig. 4. Particle size ($d$) frequency ($f$) distributions for the surface sediment and suspended matter of 10.8 m water depth for Sta. J1. The surface sample was obtained with clam grabber, and only the upper 2 cm sediments were used.

## 4.2 Estimation of settling velocity

The settling velocity of suspended matter in the bay is mainly controlled by aggregates (Van Leussen, 1988). In this case, the effective density ($\Delta\rho$) for aggregates can be derived by Eq. (1)

$$\Delta\rho = (\rho_s - \rho_w) \approx \frac{c_{tsm}}{c_V}, \qquad (1)$$

where $\rho_s$ and $\rho_w$ are densities of suspended particles and seawater; and $c_V$ values come from LISST-100 profiling data (see Table 1). Regarding the particle mean sizes as true particle diameters, the Stokes' law could yield the aggregate settling velocity:

$$w_s = \frac{gd^2(\rho_s - \rho_w)}{18\eta}, \qquad (2)$$

where $g$ is the gravitational acceleration (9.8 m/$s^2$ was adopted here); $\eta$ is the coefficient of viscosity ($1.002 \times 10^{-3}$ N·S/$m^2$ was adopted in this case); and $d$ is the particle size. Furthermore, the vertical flux could be derived from Eq. (3):

$$Q_s = w_s c_{tsm}, \qquad (3)$$

where $Q_s$ is the vertical particle fluxes within the water column. From these estimations, the flux in the surface waters of J1 is about 0.175 kg/(cm$^2$·a), while 0.121 kg/(cm$^2$·a) at the bottom of water column. The flux across the water surface of J2 is about 0.057 kg/(cm$^2$·a).

LISST-100 has the ability not only to measure the larger aggregates, but also to detect the smaller particle or single mineral. Strictly speaking, what Eq. (1) provides is not the real effective densities for the aggregates, but the approximate estimation of the mean densities. Even though, the estimations in this paper could still be used to quantify the variations of density (Mikkelsen and Pejrup, 2000). For example, the effective density of J1 is about 1 200～1 720 kg/m$^3$, which is much higher than 500～900 kg/m$^3$, the maximun effective density as Ten Brinke (1994) and Fennessy (1994) reported. These possible errors could be ascribed to the different compositions of particles, for example, the relative concentration of aggregates and single particles in the ambience. Biomass abunds in the inner bay, where effective densities vary from 343 to 403 kg/m$^3$, very close to the values of Ten Brinke (1994) and Fennessy (1994).

The particle settling velocities of J1 are about 0.97～3.98 mm/s. Both the settling velocity and flux in the inner bay are smaller than those in the outer bay (see Table 1). It is necessary to point out that Stokes' law should only be used in the static environments, i.e., under the condition of Reynold's number ($Re$) less than 1. So the settling velocities in this paper are not the real values, but an approximate calculation.

## 4.3 Analysis of beam attenuation

Beam transmission ($\tau$, %) could be determined from the LISST-100B optical detector as described by Agrawal and Pottsmith (1994). With Eq. 4, the transmission could be converted into the beam attenuation coefficient ($c$):

$$c = -\frac{1}{0.05} \times \ln\tau, \qquad (4)$$

where 0.05 m is the optical path. Many factors would affect the beam attenuation. For example, the variation of beam attenuation coefficient would contribute to the particle size distribution (Baker and Lavelle, 1984; Kitchen et al., 1982) as well as the particle concentration. These data show that beam attenuation coefficient correlate very well with the 1～250 μm volume concentration for the 1～250 μm size, and the 1～20 μm particle volume concentration, with the square ($r^2$) of correlation coefficient of 0.92 and 0.98, respectively (Fig. 5). It is inferred the 1～250 μm particle scattering is responsible for the beam attenuation, while those particles larger than 250 μm are negligible for the beam attenuation coefficient. The dry weight of suspended matters, TSM, does not exhibit any clear relationships with Beam $c$ in the Jiaozhou Bay (Fig. 5), which is quite different from the previous observations (Qin et al., 1986; Ma and Qian, 1995). This abnormality goes to several reasons. First, the spatial variations would be the foremost one. The measuring volume of LISST-100 is about 1.5 mL (laser beam cross section multiply optical path), while TSM was determined with 1 000 mL water samples. Second, the time lag between water sampling and optical profiling would contribute to the errors. Besides, Jiaozhou Bay is characterized by low turbidity and abundant organic matters, so the in-situ aggregation and disaggregation of the particles would also be responsible for the variations of particle density.

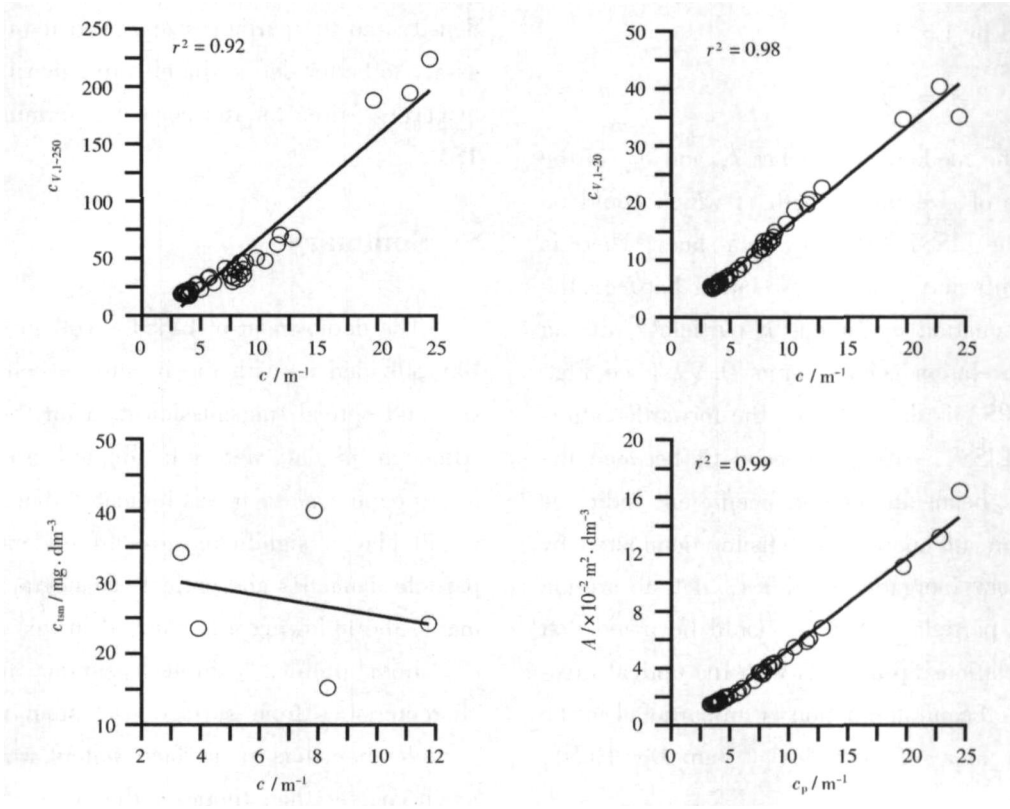


Fig. 5. Scatter plots between beam attenuation coefficient, volume concentration, projected surface area and total suspended matter.

The total beam attenuation coefficient is generally divided into three parts, attenuation ($c_w$) by sea water, absorbance ($a_{cdom}$) by CDOM (chromophoric dissolved organic matter) and attenuation ($c_p$) by particles:

$$c = c_w + a_{cdom} + c_p, \quad (5)$$

where the beam attenuation coefficient by sea water at 670 nm is almost a constant (Kitchen et al., 1982; Pak et al., 1988), and a value of 0.370 $m^{-1}$ was adopted in this paper. And parameterizations of CDOM absorption coefficient [$a_{cdom}(\lambda)$] spectrum, are typically of the form:

$$a_{cdom}(\lambda) = a_{cdom}(\lambda_0)\exp[-S(\lambda-\lambda_0)], \quad (6)$$

where $\lambda_0$ = 400 nm; $S$ is the exponential slope of spectral curves, and it equals 0.013 1 (Wu et al., 2002). Thus the absorbance coefficient of CDOM would be 0.014 08 $m^{-1}$ in the Jiaozhou Bay. And accordingly the beam attenuation coefficient by particles could be derived (see Table 1). Referring to Mikkelsen (2002b), the projected surface area can be calculated by Eq. 7:

$$A = \sum_{i=1}^{32} 1.5 \times \frac{c_{V,i}}{x_i}, \quad (7)$$

where $x_i$ is the median of size bin $i$, and $c_{V,i}$ is the concentration of size bin $i$, both of which could be found from the LISST-100 raw data sheet. There is a highly significantly linear correlation between the PSA and attenuation coefficient by particles, with an square of correlation coefficient of 0.99 (see Fig. 5). As the PSA is derived from the forward scattering data of LISST-100, the good fit between the PSA and the beam attenuation coefficient indicates that the beam attenuation is a factor dominated by scattering from inorganic particles, not absorption from organic particles. And it should be noted that this linear relationship accords with the optical theory, i.e., the beam attenuation is proportional to the cross-section area of particles (Van De Hulst, 1957).

Some other researchers have also developed similar relationships between optical properties and the PSA. Bale et al. (1994), for example, reported a power relationship between the particle cross-section and the remote sensing reflectance $R(\lambda)$ of the form $A = 25.437R(\lambda)^{1.466}$ ($r^2 = 0.897$), where the wavelength was 804 nm. Their result coincides with the optical scattering theory and empirical estimation (Forget et al., 1999; Stumpf and Pennoch, 1989). From the relationship between the attenuation coefficient by particles and the PSA, a very similar relationship could be found between the attenuation coefficient by particles and the remote sensing reflectance. Furthermore, it can be inferred that the remote sensing reflectance does not correlate with the TSM at all, which is apparently an unexpected result. Mikkelsen (2002b) indicated that the PSA could vary by up to three orders of magnitude at a constant value of the TSM (if the effective density and the particle size spctrum change). That is to say, the PSA is dependent on the TSM, the effective density and the particle sizes. And it would be necessary to better define the effective density and in-situ particle sizes for the correct determination of the TSM.

## 5 Summary

The deployment of LISST-100 in the Jiaozhou Bay provided us with the in situ suspended particle size and optical transmission data for the first time. Although the data were a bit limited in either spatial or temporal scales, it was indicated that LISST-100 would play a significant role in understanding the particle dynamics and optical oceanography. In summary, the following was reached in this study.

Both profiles exhibited similar particle size characteristics from surface to bottom waters. The particle diameters in surface waters were generally much coarser than those in the bottom areas. And the particulate components in the size range of 1～20 μm would be dominant for all the suspended matter. The volume concentration of suspended particles increases with water depth, with abrupt an increase near bottom waters. And the particles in the inner bay featured higher volume concentrations and coar-

ser grain sizes. The mean particle sizes for sediments and the suspended matter (10.8 m) at Sta. J1 were almost the same as well as their size distributions. And an affinity between these two kinds of particles could be anticipated.

On the basis of the profiling data, the suspended particle effective density varies within 340～1 720 kg/m$^3$, the settling velocity within 0.9～3.9 mm/s. The corresponding lower parameters could be found in the inner bay.

It was inferred that the optical scattering was mostly caused by 1～250 μm components, among which the particles of being less than 20 μm dominated the beam attenuation. Besides, the beam attenuation correlated with the PSA. And it was shown that the parameter of PSA could be used a proxy for the leaving reflectance estimation.

## Acknowledgements

The authors are indebted to Dr. Meng Xianwei for his invaluable comments on the manuscript. Mr. Li Chaoxin helped to deal with measurement of the sediment particle sizes in laboratory. This work was part of the MASEG (Key Laboratory of Marine Sedimentology and Environmental Geology of State Oceanic Administration, First Institute Oceanography, State Oceanic Administration) funded project "Suspended particle dynamics in coastal waters under contract No. MASEG2003003, and supported by the Qingdao Science and Technology Development Project under contract Nos 05-01-hy-83 and 05-2-JC-79.

## References

Agrawal Y C, McCave I N, Riely J B. 1991. Laser diffraction size analysis. In: Syvitski J P M, ed. Principles, Methods and Application of Particle Size Analysis. Cambridge: Cambridge University Press, 119～128

Agrawal Y C, Pottsmith H Y. 1994. Laser diffraction particle sizing in STRESS. Continental Shelf Research, 14 (10/11): 1 101～1 121

Agrawal Y C, Pottsmith H C. 2000. Instruments for particle size and settling and velocity observations in sediment transport. Marine Geology, 168 (1～4): 89～114

Baker E T, Lavelle J W. 1984. The effect of particle size on the light attenuation coefficient of natural suspensions. Journal of Geophysical Research, 89 (C5): 8 197～8 203

Bale A J, Morris A W. 1986. In situ measurements of particle size in estuarine waters. Netherlands Journal of Sea Research, 20: 183～199

Bale A J, Tocher M D, Weave R R, et al. 1994. Laboratory measurements of the spectral properties of estuarine suspended particles. Netherlands Journal of Aquatic Ecology, 28: 237～244

Burton D, Althaus M, Millward G E, et al. 1993. Processes influencing the fate of trace metals in the North Sea. Phil Trans Roy Soc (Series A), 343 (1 669): 557～568

Cheng Jiang, He Qing, Wang Yuanye. 2005. In situ estimates of floc size, effective density and settling velocity with LISST-100. Journal of Sediment Research (in Chinese), 1: 33～39

ECCB (Editing Committee on China's Bays). 1993. Records of China Bays, v. 4: South of Shandong Peninsula and Jiangsu. Beijing: China Ocean Press, 157～258

Eisma D. 1986. Flocculation and deflocculation of suspended matter in estuaries. Netherlands Journal of Sea Research, 20: 183～199

Fennessy M J. 1994. Size and settling velocity distributions of flocs in the Tamar Estuary during a tidal cycle. Netherlands Journal of Aquatic Ecology, 28: 275～282

Forget P, Ouillon S, Lahet F, et al. 1999. Inversion of reflectance spectra of nonchlorophyllous turbid coastal waters. Remote Sensing of Environment, 68: 264～272

Gartner J W, Cheng R T, Wang Peifang, et al. 2001. Laboratory and field evaluations of the LISST-100 instrument for suspended particle size determinations. Marine Geology, 175: 199～219

Gentien P, Lunven M, LeHa tre M, et al. 1995. In-situ depth profiling of particle sizes. Deep-Sea Research, 142: 1 297～1 312

Gibbs R J. 1981. Floc breakage by pumps. Journal of Sedimentary Petrology, 51: 670～672

Gibbs R. J. 1982. Floc breakage during HIAC light-blocking analysis. Environ. Sci. Technol., 298～299

Gibbs R. J., Konwar L. N. 1982. Effect of pipetting on mineral flocs. Environ. Sci. Technol., 16(2): 119～121

Gibbs R. J., Konwar L. N. 1983. Sampling of mineral flocs using Niskin bottles. Environ. Sci. Technol., 17(6): 374～375

Kitchen J. C., Zaneveld J. R. V., Pak H. 1982. Effect of particle size distribution and chlorophyll content on beam attenuation spectra. Applied Optics, 21(21): 3 913～3 918

Kurashige Y., Fusejima Y. 1997. Source identification of suspended sediment from grain-size distributions: I. Application of nonparametric statistical tests. Catena, 31: 39～52

Lan Zhigang, Gong Dejun, Yu Xinsheng, et al. 2004. Particle size correction of suspended sediment concentration measured by ADCP with in-situ particle size analyzer. Oceanologia et Limnologia Sinica, 35(5): 385～392

Ma Shubin, Qian Zhengxu. 1995. Optical study of the water masses and suspended matter distributions in the South Yellow Sea. Oceanologia Sinica (in Chinese), 26(5)(Sup): 8～15

McCandliss R. R., Jones S. E., Hearn M., et al. 2002. Dynamics of suspended particles in coastal waters (southern North Sea) during a spring bloom. Journal of Sea Research, 47: 285～302

McCave I. N. 1984. Size spectra and aggregation of suspended particles in the deep ocean. Deep-Sea Research, 31: 329～352

Mikkelsen O. A. 2002a. Examples of spatial and temporal variation of some fine-grained suspended particle characteristics in two Danish coastal water bodies. Oceanologica Acta, 25: 39～49

Mikkelsen O. A. 2002b. Variation in the projected surface area of suspended particles: implications for remote sensing assessment of TSM. Remote Sensing of Environment, 79: 23～29

Mikkelsen O. A., Hill P. S., Milligan T. G., et al. 2005. In situ particle size distributions and volume concentrations from a LISST-100 laser particle sizer and digital floc camera. Continental Shelf Research, 25: 1 959～1 978

Mikkelsen O. A., Pejrup M. 2000. In situ particle size spectra and density of particle aggregates in a dredging plume. Marine Geology, 170(3～4): 443～459

Ning Xiuren, Shi Junxian, Cai Yuming, et al. 2004. Biological productivity front in the Changjiang Estuary and the Hangzhou Bay and its ecological effects. Acta Oceanologica Sinica (in Chinese), 26(6): 96～106

Pak H., Kiefer D. A., Kitchen J. C. 1988. Meridional variations in the concentration of chlorophyll and microparticles in the North Pacific Ocean. Deep-Sea Research, 35: 1 151～1 171

Qin Yunshan, Li Fan, Zheng Tiemin, et al. 1986. Study on the suspended matters in South Yellow Sea during winter. Marine Science (in Chinese), 10(6): 1～7

Sternberg R. W., Berhane I., Ogston A. S. 1999. Measurement of size and settling velocity of suspended aggregates on the northern California continental shelf. Marine Geology, 154: 43～53

Stumpf R. P., Pennoch J. R. 1989. Calibration of a general optical equation for remote sensing of suspended sediments in a moderately turbid estuary. Journal of Geophysical Research, 94: 14 363～14 371

Sun Jun, Liu Dongyan, Wei Hao. 2003. The phytoplankton sampling and analysis strategies in the study of the Bohai Sea ecosystem dynamics. Acta Oceanologica Sinica (in Chinese), 25(Sup 2): 41～50

Ten Brinke W. B. M. 1994. In situ aggregate size and settling velocity in the Oosterschelde tidal basin (the Netherlands). Netherlands Journal of Sea Research, 32: 23～35

Trent J. D., Shanks A. L., Silver M. W. 1978. In situ and laboratory measurements o macroscopic aggregates in Monterey Bay, California. Limnology and Oceanography, 23: 626～635

Van De Hulst H. C. 1957. Light Scattering by Small Particles. New York: John Wiley & Sons

Van Leussen W. 1988. Aggregation of particles settling velocity and mud flocs—A review. In: Dronkers J., Van Leussen, eds. Physical Processes in Estuaries. New York: Springer-Verlag, 347～403

Voulgaris G., Meyers S. T. 2004. Temporal variability of hydrodynamic, sediment concentration and sediment settling velocity in a tidal creek. Continental Shelf Research, 24: 1 659～1 683

Wang Yaping, Gao Shu, Ke Xiankun. 2004. Observations of boundary layer parameters and suspended sediment transport over the intertidal flats of northern Jiangsu, China. Acta Oceanologica Sinica, 23(3): 437～448

Wang Yaping, Gao Shu, Li Kunye. 1999. A preliminary

study on suspended sediment concentration measurements using an ADCP mounted on a moving vessel. Oceanologia et Limnologia Sinica (in Chinese), 30(6): 758～763

Wu Yongsen, Zhang Shikui, Zhang Xuqin, et al. 2002. Study on the CDOM optical absorbance. Oceanologia Sinica (in Chinese), 33(4): 402～406

Yang Qingshu, Ou Suying, Xie Ping, et al. 2004. Distribution and seasonal changes of polycyclic aromatic hydrocarbons (PAHs) in surface water from Humen tidal channel. Acta Oceanologica Sinica (in Chinese), 26(6): 37～48

Zhang Minghan. 2000. Suspended matter distribution and seasonal variations in the Jiaozhou Bay. Studia Marine Sinica (in Chinese), 42: 49～54

Zhang Xiaoyu, Lin Yian, Tang Renyou, et al. 2005. Preliminary study of concentration distribution of total particulate phosphorus in estuary by remote sensing technology. Acta Oceanologica Sinica (in Chinese), 27(1): 51～56